RESEARCH ARTICLE

Disease Models & Mechanisms 6, 622-631 (2013) doi:10.1242/dmm.010512

Functional and histopathological identification of the respiratory failure in a DMSXL transgenic mouse model of myotonic dystrophy

Petrica-Adrian Panaite[1,*], Thierry Kuntzer[1,*], Geneviève Gourdon[3], Johannes Alexander Lobrinus[4] and Ibtissam Barakat-Walter[1,2,‡]

SUMMARY

Acute and chronic respiratory failure is one of the major and potentially life-threatening features in individuals with myotonic dystrophy type 1 (DM1). Despite several clinical demonstrations showing respiratory problems in DM1 patients, the mechanisms are still not completely understood. This study was designed to investigate whether the DMSXL transgenic mouse model for DM1 exhibits respiratory disorders and, if so, to identify the pathological changes underlying these respiratory problems. Using pressure plethysmography, we assessed the breathing function in control mice and DMSXL mice generated after large expansions of the CTG repeat in successive generations of DM1 transgenic mice. Statistical analysis of breathing function measurements revealed a significant decrease in the most relevant respiratory parameters in DMSXL mice, indicating impaired respiratory function. Histological and morphometric analysis showed pathological changes in diaphragmatic muscle of DMSXL mice, characterized by an increase in the percentage of type I muscle fibers, the presence of central nuclei, partial denervation of end-plates (EPs) and a significant reduction in their size, shape complexity and density of acetylcholine receptors, all of which reflect a possible breakdown in communication between the diaphragmatic muscles fibers and the nerve terminals. Diaphragm muscle abnormalities were accompanied by an accumulation of mutant DMPK RNA foci in muscle fiber nuclei. Moreover, in DMSXL mice, the unmyelinated phrenic afferents are significantly lower. Also in these mice, significant neuronopathy was not detected in either cervical phrenic motor neurons or brainstem respiratory neurons. Because EPs are involved in the transmission of action potentials and the unmyelinated phrenic afferents exert a modulating influence on the respiratory drive, the pathological alterations affecting these structures might underlie the respiratory impairment detected in DMSXL mice. Understanding mechanisms of respiratory deficiency should guide pharmaceutical and clinical research towards better therapy for the respiratory deficits associated with DM1.

INTRODUCTION

Myotonic dystrophy or dystrophia myotonica type 1 (DM1) is an autosomal dominant genetic neuromuscular disorder, that can be accompanied by abnormalities in other organs and systems with a highly variable phenotype. DM1 is caused by an expansion of a CTG repeat located in the 3′ untranslated region of the dystrophia myotonica protein kinase gene (*DMPK*) on chromosome 19q (Fu et al., 1992; Mahadevan et al., 1992). The number of repeats tends to increase from generation to generation, accounting for the genetic anticipation characteristic of this disease (Ashizawa et al., 1992; Mahadevan et al., 1992; Salehi et al., 2007). Healthy individuals have alleles with 5-35 repeats that are stably transmitted, but when this number exceeds 50, instability occurs and leads to disease. The number of CTG repeats is 50-150 in late-onset, mild DM1; 100-1000 in classic DM1; and more than 2000 in the congenital form. A significant inverse correlation is noted between onset age and repeat number and there is a general correlation between the degree of expansion and the severity of clinical manifestations (Gennarelli et al., 1996; Hunter et al., 1992).

The neuromuscular clinical manifestations of the disease include myotonia and progressive muscle weakness, with dystrophic changes in skeletal muscles including the diaphragm, cranial and limb muscles (Harper, 2001). The pathology of DM1, however, extends to other organs and systems and, as such, can be associated with several significant complications.

Respiratory and cardiac problems have long been recognized as the main complications of DM1 patients and are the major factors contributing to mortality. In fact, a study based on a cohort of 115 patients with congenital myotonic dystrophy reported that only about 50% of patients survived to their mid-30s and that the death of about 66% of surviving patients is due to respiratory causes (Reardon et al., 1993). Moreover, large cohort studies have also reported that respiratory problems are the leading cause of death (around 40%) in adult-onset DM1 (de Die-Smulders et al., 1998; Groh et al., 2008; Mathieu et al., 1999). The progressive respiratory muscle weakness leads to impairment of airway clearance, inadequate ventilation and respiratory failure (Berry et al., 1996), whereas no reduction in central airway caliber was found in the patients with the adult form of DM1 (Fodil et al., 2004). DM1 patients frequently develop pneumonia and respiratory failure as

[1]Department of Clinical Neurosciences, University Hospital, 1011 Lausanne, Switzerland
[2]Department of Fundamental Neurosciences, University of Lausanne, 1005 Lausanne, Switzerland
[3]Inserm U781, Université Paris Descartes-Sorbonne Paris Cité, Institut Imagine, 75730 Paris, France
[4]Department of Clinical Pathology, University Hospital, 1206 Geneva, Switzerland
*These authors contributed equally to this work
‡Author for correspondence (Ibtissam.Walter@unil.ch)

Received 11 July 2012; Accepted 19 November 2012

TRANSLATIONAL IMPACT

Clinical issue

The multisystemic autosomal dominant disorder myotonic dystrophy type1 (DM1), also known as Steinert disease, is the commonest form of adult-onset muscular dystrophy. DM1 is caused by abnormal expansion of CTG trinucleotide repeats in the region of *DMPK*, the gene encoding DM protein kinase. Respiratory failure is a major and potentially life-threatening feature of patients with DM1, but the pathological mechanisms of respiratory failure in DM1 are incompletely understood. Some studies suggest that the respiratory problems associated with DM1 result only from the involvement of the respiratory diaphragm muscle in progressive dystrophic and myotonic processes, whereas others suggest that the neuronal network that generates and regulates the respiratory rhythm is also involved.

Results

Because it is not feasible to take biopsies of the nervous system from patients with DM1 for histological examinations, animal models are indispensable for the study of the mechanisms underlying respiratory failure in this disease. In this study, the authors test the respiratory function and analyze the structures involved in respiratory function in DMSXL transgenic mice, an established animal model for congenital DM1 (the severest form of the disease, which develops at birth) that carries a very long CTG repeat in the *DMPK* gene. Statistical analysis of breathing function measurements shows that DMSXL mice have impaired respiratory function. Histological and morphometric analyses reveal pathological changes in the diaphragmatic neuromuscular junctions and muscle fibers of DMSXL mice and a significant decrease in the number of unmyelinated phrenic afferents. By contrast, DMSXL mice exhibit no significant neuronopathy in either cervical phrenic motor neurons or brainstem respiratory neurons.

Implications and future directions

By shedding new light on the cellular mechanisms of respiratory failure in DM1, these findings improve understanding of the main cause of death in congenital DM1. The denervation and the pathological changes of the diaphragmatic neuromuscular junctions observed in DMSXL mice suggest that a breakdown in communication between the diaphragmatic muscle fibers and the nerve endings might be the main cause of respiratory failure; the loss of phrenic unmyelinated afferents suggests that altered regulation of breathing is also involved. As well as contributing towards the understanding of respiratory failure in DM1, these findings suggest that the evaluation of respiratory parameters in DMSXL mice by non-invasive pressure plethysmography could be used to evaluate the effect of potential therapies. Moreover, future analyses of gene expression in DMSXL mice might contribute to our understanding of the molecular mechanisms involved in respiratory impairment.

a result of alveolar hypoventilation, particularly in the later stages of the disease (Bogaard et al., 1992; Jammes et al., 1986). Despite the many clinical examinations showing respiratory failure in DM1 patients, the pathological mechanisms underlying this failure are still not completely known. Several studies suggest that the causes of respiratory failure are varied and could be due either to the involvement of respiratory muscles in the dystrophic and myotonic process (Bégin et al., 1980; Bogaard et al., 1992; Jammes et al., 1985; Serisier et al., 1982; Zifko et al., 1996) or to abnormalities in the nervous system, which generates and controls breathing drive (Kilburn et al., 1959; Ono et al., 1996; Takasugi et al., 1995).

In neurodegenerative diseases in humans, access to affected tissue is generally limited to the end-stage of the disease and to biopsies, making animal models extremely useful (Gomes-Pereira et al., 2011; Wansink and Wieringa, 2003). In the present study, we have used DMSXL transgenic mice. These mice express the *DMPK* gene in a variety of tissues with a pattern similar to the patterns of the murine *Dmpk* gene in mice and the *DMPK* gene in human tissues (Huguet et al., 2012). To address whether the DMSXL transgenic mice animal model, which carry a long CTG repeat and display DM1 features (Gomes-Pereira et al., 2011), have respiratory problems, we tested and compared the breathing function in DMSXL and control mice. To identify the pathological changes underlying any respiratory complications, we analyzed the diaphragm muscle and the neural network that generates, controls and transmits the respiratory rhythm.

RESULTS

Impaired respiratory function in DMSXL mice

To investigate whether the DMSXL transgenic mice have respiratory alterations, we first measured, under the same conditions, the most relevant respiratory parameters in awake young or adult DMSXL and control (wild-type and DM20) mice. The analysis of breathing patterns (Fig. 1) and parameters recorded in young awake mice (2 months old) revealed a small but significant decrease in tidal volume (TV) and volume per minute (minute volume, MV) in DMSXL mice.

We noticed that awake mice, especially the DMSXL mice, appeared highly stressed and agitated during recording, and so we assessed the respiratory function in anesthetized mice. The results of these experiments showed that in 2-month-old anesthetized mice, the respiratory rate (RR) and the TV were significantly decreased in DMSXL mice compared with control mice taken from the same litter and with DM20 mice that do not express the DM1 phenotype (wild type and DM20). Consequently, the mean value for minute volume/body weight (tidal volume × breathing frequency/body weight) was also reduced in DMSXL mice (Table 1). In addition, a significant reduction was detected in arterial blood oxygen saturation (SpO_2) in DMSXL mice. Overall, we found that alterations in respiratory function observed in young DMSXL mice did not really change as a function of age. In fact, measurement of respiratory parameters in 6-month-old mice confirmed the decrease in RR, TV, MV and SpO_2 in DMSXL mice (Table 2). To be sure that the alterations in respiratory pattern observed in DMSXL mice are not related to their small size, we measured the respiratory function in wild-type mice having similar size and weight (24±0.6 g). The results of these experiments showed no changes in RR and in SpO_2 in the small control mice compared with normal control mice (RR, 135.7±8.2 in small control versus 126±15.1 in normal control; SpO_2, 98.23±0.21 versus 98.62±0.38).

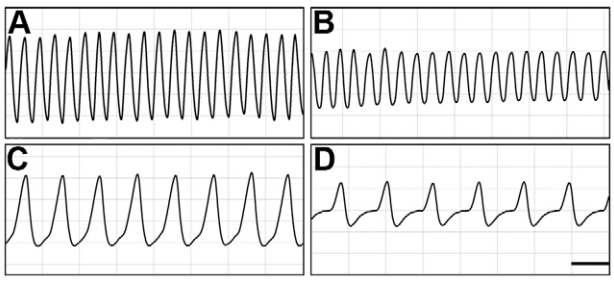

Fig. 1. Typical breathing patterns. Representative recordings showing typical examples of breathing patterns over a 4-second snapshot in 6-month-old awake (A,B) and anesthetized (C,D) wild-type (A,C) and DMSXL mice (B,D). Scale bar: 0.5 seconds.

Table 1. Mean values of respiratory parameters in 2-month-old anesthetized wild-type and DM1 transgenic mice

Respiratory parameter	Wild-type mice (BW=28.5±0.6 g)	DM20 mice (BW=28.0±0.8 g)	DMSXL mice (BW=20.2±0.8 g)	*P*1	*P*2	*P*3
RR (breaths/minute)	126.2±15.1	124.5±18.6	86.2±7.6	ns	<0.01	<0.05
TV (ml)	0.312±0.024	0.281±0.046	0.226±0.034	ns	<0.01	<0.01
MV (ml)	39.61±7.82	35.05±5.76	19.43±2.68	ns	<0.01	<0.05
TV/BW (ml/g)	0.011±0.001	0.010±0.001	0.011±0.001	ns	ns	ns
MV/BW (ml/g)	1.43±0.23	1.25±0.19	0.96±0.14	ns	<0.01	<0.05
SpO_2 (%)	98.62±0.38	97.85±1.13	94.23±1.47	ns	<0.01	<0.01
HR (beats/minute)	574±48	630±64	619±40	ns	ns	ns

Values are mean ± s.d.; *n*=5. HR, heart rate; BW, body weight; *P*1, comparisons between wild-type and DM20 mice; *P*2, comparisons between wild-type and young DMSXL mice; *P*3, comparisons between DM20 and young DMSXL mice; ns, non-significant.

This result ruled out the possibility that the respiratory alterations observed in DMSXL mice are caused by their small size. Moreover, the comparison and statistical analysis of all our results revealed two points: first, the breathing function in DM20 transgenic mice, which do not express the phenotype of DM1 disease, was similar to that in wild-type mice; and second, anesthesia caused a reduction in breathing parameters in all mice compared with awake mice.

Pathological changes in diaphragmatic muscle fibers and neuromuscular junctions

To assess whether modifications in the diaphragm are responsible for the impairment in respiratory function in DMSXL mice, we first examined diaphragm sections stained for either ATPase activity or with hematoxylin and eosin (H&E). In both control (wild type and DM20) and DMSXL mice, we observed that the majority of fibers did not show phosphorylase activity and were only counterstained with Luxol Fast Blue (>85% type II); a small number of fibers were strongly stained (type I) (Fig. 2). However, quantification of muscle fibers showed an increase (14.7%) in the mean percentage of type I fibers in DMSXL mice compared with control mice. Other dystrophic alterations were observed in DMSXL diaphragm sections, such as centrally located nuclei, an increase in interfasicular connective tissue and the presence of infiltrating inflammatory cells (Fig. 2). The abnormality of DMSXL diaphragm muscle was accompanied by an accumulation of DMPK RNA with its expanded CUG repeat, found as foci in the nuclei of muscle fibers (Fig. 3). About 58% of DMSXL diaphragm muscle fiber nuclei contained between one and seven foci, with an average of 2.2 foci per affected nucleus. No nuclear RNA foci were detected in the diaphragm muscle fibers of control mice.

The diaphragm neuromuscular junctions (NMJs) also underwent pathological changes in DMSXL mice. Despite the presence of bundles of axons in the serial muscle sections, about 20% of the endplates were denervated and had no contact with nerve terminals. Moreover, numerous EPs exhibited lengthened shapes and faint labeling compared with controls (Fig. 4). Statistical analysis of the morphometric results confirmed the abnormality of EPs in DMSXL mice. A significant decrease in mean EP area (11%) and shape complexity (16.3%) was found in DMSXL mice, as well as in the density of acetylcholine receptors (AChRs) on postsynaptic membranes (reduced by 19.9%; Fig. 4). Combined staining with α-BTX and FISH (see Materials and Methods) revealed that several foci were located in sub-synaptic nuclei.

Table 2. Mean values of respiratory parameters in 6-month-old anesthetized wild-type and DM1 transgenic mice

Respiratory parameter	Wild-type mice (BW=33.8±3.6 g)	DMSXL mice (BW=22.2±2.0 g)	*P*
RR (breaths/minute)	125.7±14.4	87.8±5.3	<0.01
TV (ml)	0.381±0.041	0.228±0.013	<0.01
MV (ml)	47.72±11.01	20.48±1.33	<0.01
TV/BW (ml/g)	0.011±0.001	0.010±0.001	<0.01
MV/BW(ml/g)	1.4±0.17	0.94±0.09	<0.05

Values are mean ± s.d.; *n*=5. BW, body weight; ns, non-significant.

Severe loss of phrenic nerve unmyelinated axons

Light microscopy revealed no obvious morphological differences between control (wild type and DM20) phrenic nerve transverse sections of DMSXL mice, except for the smaller size of DMSXL nerve sections. In all animals, the phrenic nerve consisted of a single fascicle containing myelinated and unmyelinated axons. In electron microscopy analysis, apart from some pathological signs (aberrant Schwann cell proliferation, increased number of macrophages) observed on DMSXL thin nerve sections, a severe and significant loss (41%; $P<0.01$) in the number of unmyelinated axons was found (Fig. 5). By contrast, the number of myelinated fibers showed a slight but not significant decrease (5%; $P=0.30$), although the thickness of myelin sheath was reduced significantly ($P<0.01$) in DMSXL mice compared with controls (628±9 nm versus 770±54 nm). FISH analysis showed that several Schwann cells that intermingled with axons contained one or two ribonuclear foci in their nuclei (Fig. 5).

Absence of significant alterations in phrenic motor or brainstem respiratory neurons in DMSXL mice

Histological examination of cervical phrenic motor neurons showed rare apoptotic features (nuclear eccentricity, loss of Nissl bodies or cytoplasm granulation). The estimation of the number of neurons by the physical disector method revealed a slight but not significant decrease (5%; $P=0.13$) in the mean number of cervical phrenic motor neurons in DMSXL mice. In addition, only a few mRNA foci were observed in phrenic motor neurons in DMSXL mice.

The histological and morphometric analysis of five brainstem disector pairs containing respiratory neurons located in a region that extends from the compact portion of the nucleus ambiguus to just behind the facial motor nucleus (Fig. 6) ruled out the presence of neuronopathy in DMSXL mice respiratory neurons. In

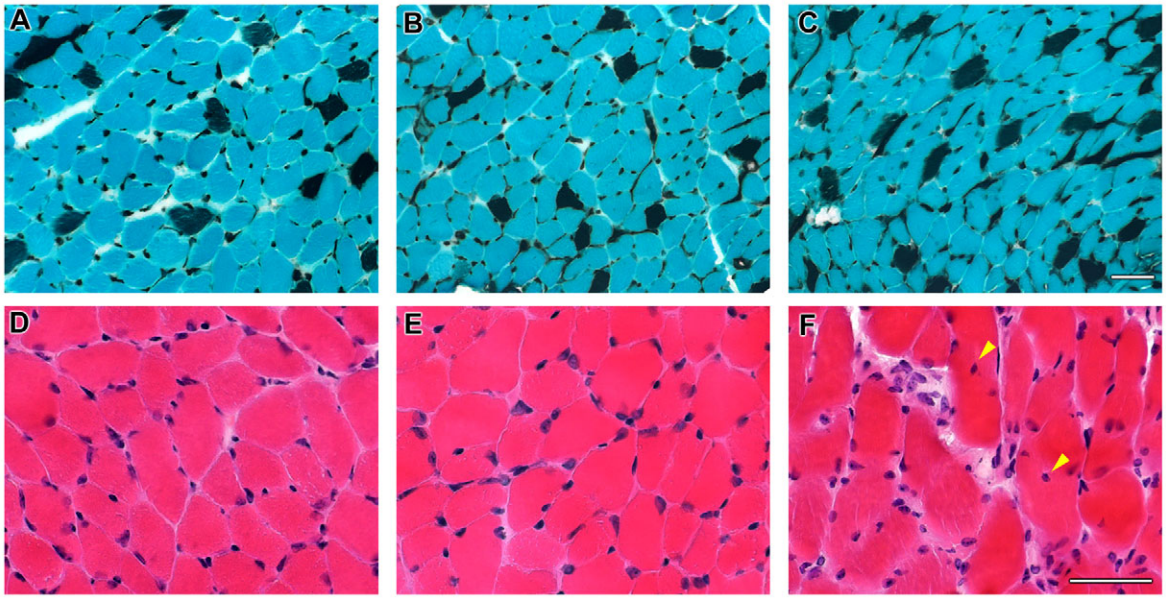

Fig. 2. Cross-diaphragm muscle sections of 2-month-old mice. Wild-type (A,D), DM20 (B,E) and DMSXL (C,F) mice were labeled either for myofibrillar ATPase activity after pre-incubation at pH 4.2 (A-C), or with H&E (D-F). On ATPase-stained sections, two main fiber types can be observed in control and DMSXL mice. (A,B) In wild-type and DM20 control mice, there are 90% ATPase unstained fibers (fast-twitch type II fibers), only stained with Luxol Fast Blue, and 10% are ATPase darkly stained fibers (slow-twitch type I fibers). (C) In DMSXL mice, a slight increase (11.5%) in the number of fast-twitch type I fibers was counted. (D-F) Diaphragm muscle sections were taken from wild-type and DM20 control mice (D,E) and DMSXL mice (F) stained with H&E. The presence of interfasicular connective tissue, inflammatory cells and central nucleated fibers (arrowheads) can be easily observed on DMSXL sections (F). Scale bars: 50 μm.

fact, the histological examination of respiratory neurons located in the area of the ventrolateral nucleus of the solitary tract and neurons scattered in the vicinity of the nucleus ambiguus and the surrounding reticular formation did not reveal apoptotic features. Moreover, the physical disector estimation of neuron density showed only a non-significant reduction (3%) in the density of DMSXL respiratory neurons as compared with controls.

DISCUSSION

The major result provided by this study is the demonstration that DMSXL mice, a transgenic mouse model of DM1, have respiratory impairments characterized by a significant decrease in RR, TV, MV and SpO_2 compared with control mice. The second important result is the detection of a partial denervation of diaphragmatic EPs and significant pathomorphological changes in diaphragm EPs and muscle fibers in DMSXL mice, which indicate a possible breakdown in communication between the diaphragmatic muscles fibers and the nerve terminals. Also, a severe and significant loss in the number of phrenic unmyelinated afferents was detected in DMSXL mice, whereas no significant alterations were observed in phrenic motor neurons or brain stem respiratory neurons.

Taking into consideration that the diaphragm muscle is the principal respiratory muscle and that afferent phrenic unmyelinated fibers are involved in control of the basic respiratory rhythm, we believe that the pathological changes observed in the diaphragm and phrenic nerve afferents in DMSXL mice are responsible for the respiratory failure assessed in these mice. Because central neurons did not show significant neuronopathy, the generation of the breathing rhythm is probably not affected in DMSXL mice.

Impaired respiratory function in DMSXL mice

For the study of mechanisms of myotonic dystrophy diseases, there is a growing use of various animal models (Gomes-Pereira et al., 2011; Wansink and Wieringa, 2003). Consequently, some of the same techniques used in the clinic to examine patients should be adapted for analysis in animal models. Several studies reported that pressure plethysmography can serve as a valuable respiratory function test in conscious or anesthetized small animals. This non-invasive method is particularly appropriate for quick and repeatable screening of respiratory function over short and extended periods of time for large numbers of mice and rats. Moreover, the intra-individual variability in respiratory function measured by pressure plethysmography is acceptable (Huang et al., 2011; Stunden et al., 2001; Yilmaz et al., 2005). Therefore, in the current study we used pressure plethysmography to assess the respiratory function in DMSXL and control mice. The comparison and the statistical analysis of several breathing measurements demonstrated a significant decrease in most relevant respiratory parameters in anesthetized DMSXL mice, indicating an impairment in breathing function in young and adult mice. Because alterations in the breathing parameters observed in young mice do not become more severe in adult animals, we inferred that respiratory impairment in DMSXL mice does not depend on the age of the animals. We also demonstrated that respiratory changes including RR and SpO_2 were not related to the small weight of the DMSXL transgenic mice. In addition, the hypothesis that the respiratory abnormalities observed in these mice are due to overexpression of the genes carried by the transgene is excluded because the DM20 transgenic mice carrying the same transgene but with a normal number of CTG repeats did not show alterations in respiratory function compared with wild-type mice.

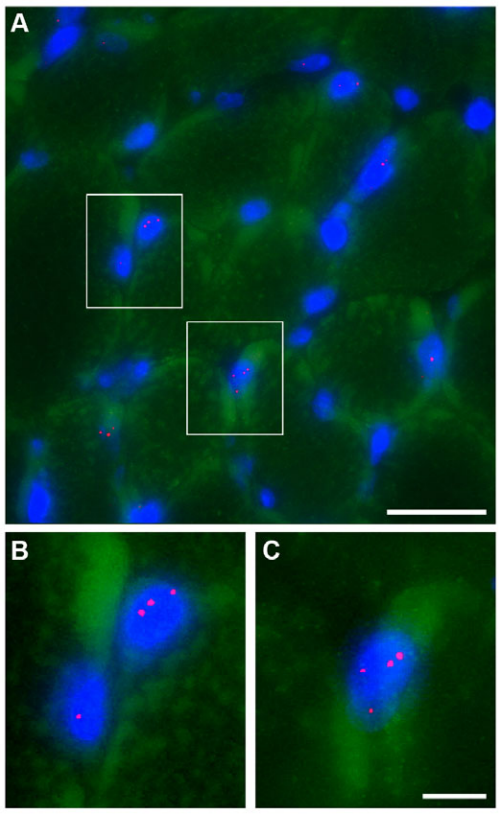

Fig. 3. Detection of nuclear foci by FISH on frozen sections of diaphragm muscle prepared from 2-month-old DMSXL mice. Using the Cy3-labeled CAG-repeats PNA-probe, the RNA inclusions are labeled in red within the nuclei of muscle fibers stained in blue with DAPI. (A) Low magnification image shows numerous nuclei stained in blue surrounding the diaphragm muscle fibers. (B,C) At higher magnification the presence of one or more foci inside the nuclei is easily observed. Scale bars: 20 µm (A); 5 µm (B,C).

Statistical analysis of the results of several recordings showed that the mean values of respiratory parameters in anesthetized mice were reproducible and comparable with values previously reported (Daubenspeck et al., 2008; Hamelmann et al., 1997; Hoymann, 2007; Huang et al., 2011). Several studies reported that the breathing frequency decreases by about 40-60% in anesthetized mice compared with conscious mice (Hamelmann et al., 1997; Takezawa et al., 1980). In our study, the RR and MV were decreased under anesthesia to about 47% in controls and 34% in DMSXL mice compared with conscious animals, which indicates that DMSXL mice are more sensitive to anesthesia. In agreement, clinical reports have mentioned that, in general, patients with DM1 disease present potential respiratory depression during or after anesthesia, although the mechanisms underlying the anesthesia effect on respiratory depression in DM1 patients is not well investigated (Ogawa et al., 1993; Yomosa et al., 1991). It is conceivable that in DMSXL mice anesthesia acts directly on the neural network that generates, controls and transmits the respiratory rhythm and also acts on the diaphragm, which is the main respiratory muscle. Another possibility is that the anesthesia has an effect on several areas of the central nervous system, which in turn exert an influence on the structures involved in respiratory function.

Because DMSXL mice displayed impairment in respiratory function, these mice present a useful tool for investigating the pathological changes underlying the respiratory failure associated with DM1 disease. Importantly, the evaluation of respiratory parameters by non-invasive pressure plethysmography could be used to evaluate the effect of potential therapies in DMSXL mice.

Role of pathological changes in the DMSXL diaphragm in respiratory impairment

Anatomical and electrophysiological data suggest that the basic breathing rhythm of higher mammals is generated and regulated in brainstem respiratory neurons. Then, the stimuli are transmitted via cervical phrenic motor neurons and phrenic nerves to the diaphragmatic muscle, which is the principal respiratory muscle (Ramirez et al., 2002). Therefore, the impairment in respiratory function observed in DMSXL mice might have a central origin in decreased respiratory drive, or a peripheral origin such as weakness of the diaphragmatic muscles, or both.

Because diaphragmatic muscle is the only effective respiratory muscle pump and its action contributes to more than 66% of the TV (Mead et al., 1995; Singh et al., 2003), our efforts were focused on analyzing diaphragm muscle fibers and NMJs. Several of the alterations observed in DMSXL diaphragm muscle lead us to believe that they might cause, at least partially, the respiratory failure in these mice. In fact, the increase in histochemically defined type I muscle fibers, the presence of central nuclei, the gain in interfasicular connective tissue and inflammatory cells, as well as the accumulation of expanded CUG mRNA in muscle fiber nuclei all indicate that the diaphragm muscle of DMSXL mice is involved in the dystrophic processes. This assumption can be supported, on the one hand, by the presence of similar histopathological changes in biopsies of DM1 patients (Harper, 1989; Romeo, 2012) and, on the other hand, by the changes in fiber type composition of the diaphragm muscles in an animal model of Duchenne muscular dystrophy, which is characterized by severe muscle degeneration (Guido et al., 2010; Petrof et al., 1993). These authors hypothesize that the progressive changes in fiber type probably permit better adaptation of the muscle to its function during progression of the disease. It is possible that the increased number of type I diaphragm fibers (slow-twitch) in DMSXL mice, due to a selective degeneration of type II fibers (fast-twitch), probably causes alterations in diaphragmatic muscle function in these mice.

The detection of an accumulation of CUG expanded RNA as foci in diaphragm muscle fiber nuclei is another indication of the abnormality of the DMSXL diaphragm. The presence of foci and the sequestration of muscleblind protein in the nuclei diaphragm NMJs has also been reported in DM1 muscle biopsies and in another DM1 transgenic mouse model (Wheeler et al., 2007). It is well known that the main pathogenic process at the base of DM1 is a toxic RNA gain-of-function effect of mutant DMPK transcripts, which are retained in distinct ribonuclear foci within the cell nuclei. Taking into consideration this hypothesis, inferring that these nuclear foci sequester essential proteins and disrupt their normal function in the cell (Kuyumcu-Martinez and Cooper, 2006; Nykamp and Swanson, 2008; Querido et al., 2011), we can hypothesize that nuclear retention of mutant *DMPK* mRNA in diaphragmatic muscle fibers alters the function of the diaphragm, which can lead to respiratory failure.

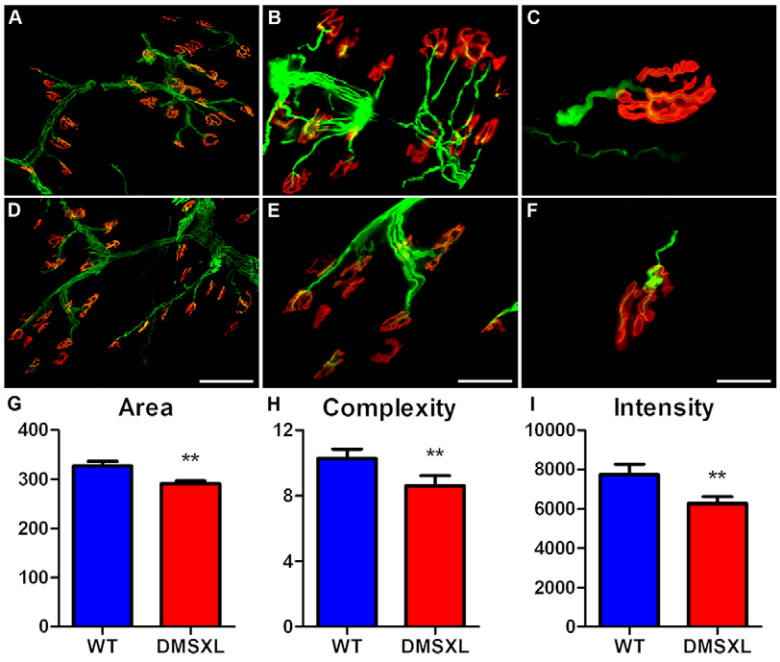

Fig. 4. Pathological changes in neuromuscular junctions of DMSXL mice. (A-F) Representative micrographs of diaphragm muscle cryostat sections that were stained with rhodamine α-BTX (red) and neurofilament antibody (green). (A-C) In wild-type control mice practically all the EPs are innervated by branches of axons. (D-F) In DMSXL mice, EPs with no contact to axon terminals are easily identified. (C,F) A single EP is shown at higher magnification. In DMSXL mice (D-F), the EPs have smaller size and less complex shape than in control mice (A-C). The mean surface area of EPs, the shape complexity and the density of acetylcholine receptors on post-synaptic membranes labeled with rhodamine α-BTX are represented in the three histograms. More than 1500 EPs were measured from each mouse line (n=7). Statistical analysis of the results reveals that all three parameters are significantly (**P<0.01) smaller in DMSXL mice compared with wild-type control mice. Scale bars: 100 μm (A,D); 50 μm (B,E); 20 μm (C,F).

In DMSXL mice, the diaphragmatic NMJs also undergo pathological changes. About 20% of diaphragm EPs were denervated and the area and the shape complexity of EPs were significantly reduced. Moreover, the AChR density on postsynaptic membranes was significantly lower. It should be noted that in previous experiments in DM1 transgenic mice carrying only 500 CTG repeats we detected similar abnormalities in the structure of diaphragmatic EPs (Panaite et al., 2008). The fact that the statistical analysis revealed that the pathological changes in diaphragmatic EPs found in DMSXL mice, carrying about 1300 CTG repeats, do not vary significantly from those observed in DM1 mice indicates that there is no relationship between the severity of EP alterations and length of the CTG repeat. This is consistent with clinical studies reporting that some DM1 features such as cataract, sleep disorders, gastrointestinal problems, respiratory insufficiency and cardiac abnormalities do not correlate with the size of the unstable base CTG triplet (Jaspert et al., 1995; Marchini et al., 2000).

It is quite possible that the denervation and abnormalities seen in EP structure are induced by the loss of 5% of phrenic myelinated fibers and also by the alterations affecting muscle fibers. A recent study reported that one of the mechanisms underlying the impairment of neuromuscular connections observed in DM1 tissue cultures is the misexpression of two members of the *SLITRK* family genes, which are involved in neurite outgrowth, neuritogenesis and synaptogenesis (Marteyn et al., 2011).

Because the normal function of the diaphragm in both inspiratory and expiratory phases of breathing requires neural stimulation via normal NMJs, the damage and alterations to the phrenic nerve affect the diaphragmatic DMSXL NMJs and probably results in failure of action potential transmission (Andreose et al., 1995; Kumai et al., 2005). Numerous clinical data report that patients with signs of muscular weakness and myotonia also show respiratory impairment (Bégin et al., 1997; Jammes et al., 1985; Serisier et al., 1982; Zifko et al., 1996), therefore, the pathological changes observed in DMSXL diaphragm muscle are probably sufficient to affect the normal function of the diaphragm during breathing in these mice.

Role of alterations in phrenic afferents in breathing impairment in DMSXL mice

In addition to the motor function, the phrenic nerve is also rich (43%) in afferent axons composed mainly of unmyelinated axons. The motor component of the phrenic nerve is mainly myelinated whereas the sensory component is mainly unmyelinated (Langford and Schmidt, 1983). The thin afferent fibers are believed to be connected to polymodal receptors on the surface of the muscle and within the muscle. Free nerve endings located in muscle are presumed to represent these receptors (Brown and Fyffe, 1978; Duron and Marlot, 1980; Goshgarian and Roubal, 1986; Kumazawa and Mizumura, 1977). Groups of these fibers are activated principally by chemical stimuli rather than by mechanical stimuli (Kumazawa and Mizumura, 1977).

The tracer combination of the anterogradely transported Fast Blue and the retrogradely transported Nuclear Yellow allowed the demonstration that some phrenic nerve afferents terminate at the C4 and C5 spinal cord in rats (Revelette et al., 1988). Other afferents project to the brain stem nuclei, including dorsal respiratory group neurons (DRG) and ventral respiratory group neurons (VRG) (Larnicol et al., 1985; Macron et al., 1985; Marlot and Duron, 1981). The neurons in the DRG and VRG in the brain stem are primarily responsible for the generation of the rhythmic pattern of respiration. However, there is growing evidence that diaphragmatic afferent stimuli exert a modulating influence on the basic respiratory rhythm, although they do not play a crucial primary role in generating or maintaining the rhythm.

Electrical stimulation of phrenic nerve afferents during inspiration produce a premature transition from the inspiratory to expiratory phase, and it was concluded that phrenic afferents exert

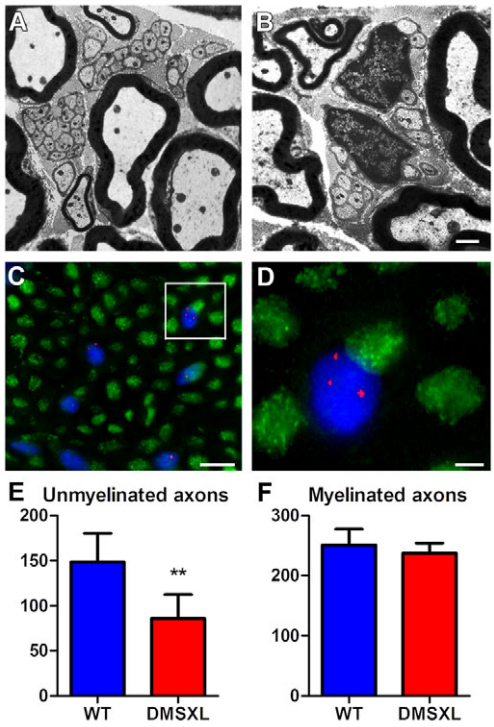

Fig. 5. Pathological changes in phrenic nerves of DMSXL mice. (A,B) Representative electron micrographs of ultrathin transverse phrenic nerve sections taken from 6-month-old wild-type (A) and DMSXL transgenic mice (B). On sections from control mice, numerous unmyelinated axons surrounded by a Schwann cell can be observed (A), whereas on the DMSXL mice section (B) the presence of unmyelinated axons is less frequent than in control mice. (C,D) On frozen sections prepared from DMSXL phrenic nerve, the FISH combined with neurofilament immunostaining demonstrates the presence of CUG RNA foci (red) in Schwann cell nuclei (blue), which are intermingled with the axons (green). (E,F) Histograms show the mean number of unmyelinated fibers (E) and myelinated fibers (F) counted on ultrathin phrenic nerve sections taken from seven wild-type mice and seven DMSXL mice. $^{**}P<0.01$. Scale bars: 1 µm (A,B); 10 µm (C); 2 µm (D).

an inhibitory influence on inspiratory motor drive (Jammes et al., 1986; Marlon et al., 1988). However, other studies report that the activation of small-fiber afferents in the diaphragm of anesthetized dogs induces a marked excitatory effect on phrenic motor neurons and brain stem respiratory neurons (Revelette et al., 1988; Speck and Revelette, 1987). These studies concluded that the phrenic nerve afferent populations are capable of producing at least two distinct effects: a net excitation of inspiratory activity at the pre-motor level and a strong inhibitory effect on motor output at the spinal level.

In our current study, the statistical analysis of morphometric results showed a severe loss of unmyelinated phrenic afferents (>40%), whereas phrenic myelinated fibers undergo a slight and non-significant reduction (5%). Furthermore, the phrenic motor neurons and the brainstem respiratory neurons do not suffer from significant neuronopathy because only a small non-significant loss in the number of neurons was found. With reference to the data reported in the studies mentioned above, we can deduce that in DMSXL mice the afferent feedback is reduced and the regulation of respiratory drive is altered, whereas the generation of breathing rhythm is probably not affected.

In summary, despite the large cohort studies showing that respiratory problems are the leading cause of death, especially in surviving patients with congenital DM1 (Reardon et al., 1993), and to a lesser degree in adult-onset DM1 (de Die-Smulders et al., 1998; Groh et al., 2008; Mathieu et al., 1999), the pathological mechanisms underlying respiratory failure are still not completely known.

Our study in a transgenic mouse model of DM1 sheds light on possible mechanisms of respiratory failure, because the respiratory impairments seen in these mice are caused by pathological changes affecting mainly the diaphragm respiratory pump and phrenic unmyelinated afferents. Because cervical phrenic motor neurons and brainstem respiratory neurons do not show significant neuronopathy, the generation of the breathing rhythm is probably not affected in DMSXL mice.

MATERIALS AND METHODS

All experiments were carried out in accordance with the local veterinary guidelines for care and use of experimental animals and all analyses and counts were performed blinded to the animal genotype.

Generation of the DM1 animal model

The generation of transgenic mice carrying the human genomic DM1 region with expanded repeats of either ~500 CTG (DM1 mice; displaying mild DM1 phenotype) or 20 CTG (normal; do not develop DM1 phenotype) has been described previously (Gantelet et al., 2007; Seznec et al., 2001). DMSXL mice carrying more than 1300 CTG were obtained from DM1 mice, after large expansions of the CTG repeat over successive generations (Gomes-Pereira et al., 2007; Panaite et al., 2011). Expression of expanded CUG leads to the formation of numerous foci that co-localize with muscleblind-like protein 1 and 2 (MBNL1 and MBNL2). Mild missplicing of target RNA is observed in muscles and heart tissues. These molecular features of DM1-associated RNA toxicity were associated with high mortality, growth retardation and muscle defects (abnormal histopathology, reduced muscle strength and lower motor performances) (Huguet et al., 2012).

Heterozygous mice, homozygous and wild-type mice are obtained by breeding from the same litter. Only homozygous transgenic mice were used in our study because the heterozygous mice expressing a low level of DMPK transcripts do not have an obvious phenotype. Thirty mice were used: group 1 consisted of five 2-month-old DMSXL mice and five control mice taken from the same litter (body weight 20.2±1.1 g versus 27.6±0.8 g); group 2 consisted of five 2-month-old DM20 mice and five control mice (body weight 28.0±0.6 g versus 28.5±0.8 g); and group 3 consisted of five 6-month-old DMSXL mice and five control mice (body weight 22.0±2.0 g versus 33.8±3.6 g).

Respiratory function analysis (pressure plethysmography protocol)

To investigate whether the DMSXL mice have respiratory failure, we measured the breathing function in DMSXL and control mice using pressure plethysmography (Respiromax system, Columbus Instruments, Columbus, OH), a precise method adapted for both awake and anesthetized small animals (Stunden et al., 2001; Yilmaz

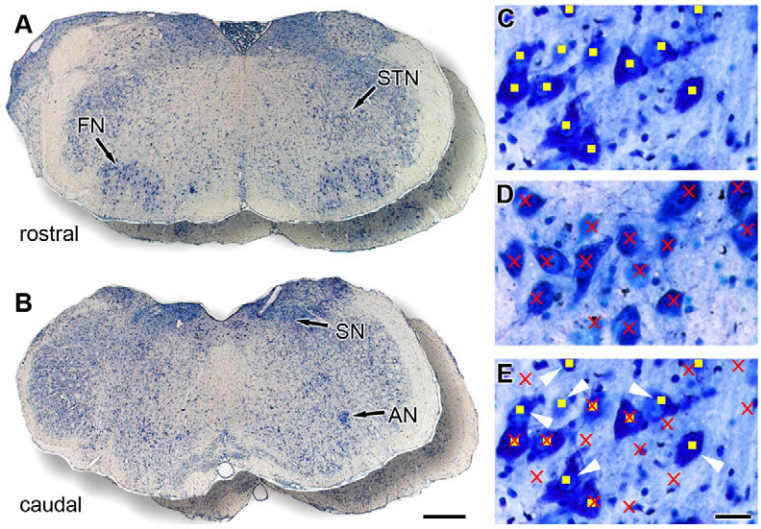

Fig. 6. Analysis of brainstem respiratory nuclei by the physical disector method. (A,B) Caudal and rostral disector pairs. The density of respiratory neurons located in a region extending from the nucleus ambiguus (caudal disector pair sections) and facial motor nucleus (rostral disector pair sections) was estimated by the physical disector method. Five disector pairs were analyzed from each animal (*n*=5). (C-E) The two sections of a dissector pair were overlaid one on top of the other using Adobe Photoshop CS5 and carefully aligned using common landmarks (general contour, brain stem nuclei, blood vessels, etc); then the neurons present in the front (C) and back (D) sections were marked with two different types of symbols. The set of symbols from the back section were superimposed on the ones from the front section (E) and the neurons present only in the front but not in the back section were counted and used to estimate the density of neurons. AN, nucleus ambiguus; FN, facial nucleus; SN, solitary tract nucleus; STN, spinal tract of the trigeminal nerve nucleus. Scale bars: 500 μm (A,B); 25 μm (C-E).

et al., 2005). Individual mice were first weighed then placed in a respiromax cylindrical chamber. A tail rod was moved forward until it secured the animal, preventing it from backing up and maintaining a prone position. The head of the animal emerged through an inflatable latex cuff into a head chamber and the neck cuff was pressurized to seal the body chamber. Each mouse was allowed to acclimatize to the plethysmography chamber for ~5 minutes before tests began. A sensitive transducer measured the changes in pressure in the body chamber caused by the animal's respiration. Signals from the pressure transducer were amplified and digitized by a respiratory function software (Columbus Instruments), displayed and stored in a computer for graphical and statistical analysis. In all experiments, the temperature of the body chamber was continuously monitored using a thermal probe. The following parameters were evaluated: tidal volume (ml), respiratory rate (breaths/minute), minute volume (tidal volume multiplied by respiratory rate, ml/minute). The respiratory function of each mouse was tested several times over a period of 2 weeks.

In another series of experiments, the respiratory function was measured in mice anesthetized with isoflurane using a Matrx Quantiflex low flow V.M.C. anesthesia system (Midmark, Versailles, OH). The animals were placed individually in an induction chamber and anesthesia was induced with 5% isoflurane in a gas mix of O_2/N_2O_2 (30/70%). The animals were then quickly placed inside the Respiromax system, with a 1.5% isoflurane flow in the head chamber in the same O_2/N_2O_2 gas mix. A MouseOx pulse oximeter (Starr Life Sciences, Oakmont, PA) was placed on the upper, right hindleg of each mouse to measure the oxygen saturation of arterial hemoglobin (SpO_2) and heart rate; the body chamber was closed and the neck cuff swollen. Animals were allowed to settle for 5 minutes before the first set of measurements.

Animal perfusion and tissue preparation

After testing the respiratory function, mice were deeply anesthetized and the brainstem, cervical spinal cord, right and left phrenic nerves and diaphragm muscles carefully removed from each animal as previously described (Panaite et al., 2008; Panaite et al., 2011).

Analysis of diaphragm muscle sections

To examine diaphragm muscle fibers, 10-μm thick transverse cryostat sections were prepared and myofibrillar adenosine triphosphatase (ATPase) activity assessed after pre-incubation at pH 4.2 (Sheehan and Hrapchak, 1980) followed by counterstaining with Luxol Fast Blue. Other sections were stained with hematoxylin and eosin (H&E). The number of each fiber type was assessed using an image-processing program (ImageJ 1.40, National Institutes of Health, Bethesda, MD). To analyze the NMJs, serial longitudinal cryostat sections (20-μm thick) of diaphragm muscle were double labeled with tetramethylrhodamine-conjugated α-bungarotoxin (α-BTX; Invitrogen, Life Technologies, Carlsbad, CA,) and with a primary polyclonal antibody directed against the 200-KDa neurofilament protein (AB1982, Millipore, Billerica, MA).

Muscle sections were observed under a Zeiss AxioPlan 2 microscope (Zeiss; Oberkochen, Germany), photographed using an image-acquisition program (Zeiss AxioVision with Axiocam HRc) and images systematically analyzed in the ImageJ 1.40 program. The percentage of denervated endplates (EPs) was estimated and the morphometric parameters (area, shape complexity and fluorescence intensity of rhodamine-α-BTX labeling) of each EP were measured and calculated as described in our previous studies (Panaite et al., 2008; Panaite et al., 2011). More than 1500 EPs were measured from each mouse line (*n*=7 DMSXL and control mice).

Detection of nuclear RNA foci

Fluorescence *in situ* hybridization (FISH) was performed on 7-μm thick frozen sections as described by Guiraud-Dogan et al. (Guiraud-Dogan et al., 2007). In short, sections of diaphragm muscle, phrenic nerve, cervical spinal cord and brain stem were dried, fixed, then incubated in 30% (v/v) formamide and 2× standard sodium citrate (SSC) for 10 minutes, hybridized with the PNA probe Cy3-OO-CAGCAGCAGCAGCAG (1 ng/μl) (Eurogentec, Liège, Belgium) for 2 hours at 37°C in buffer [30% (v/v) formamide, 2× SSC, 0.02% (w/v) BSA, 66 μg/ml yeast tRNA (Invitrogen) and 2 mM vanadyl complex (Sigma-Aldrich, St Louis, MO)]. Sections were then washed for 30 minutes in 30%

(v/v) formamide and 2× SSC at 50°C and then for 30 minutes in 1× SSC at 20°C. Nuclei were stained by incubating with DAPI for 15 minutes at room temperature. The cervical spinal cord, phrenic nerves and brain stem sections were additionally labeled with polyclonal anti choline-acetyltransferase antibody (ChAT, 1:50; AB144P, Millipore) as previously described (Panaite et al., 2011).

Analysis of phrenic nerve sections

For light microscopy analysis, semithin transverse sections (1 μm) were cut at different levels from phrenic nerve trunks and stained with Toluidine Blue. For electron microscopy examination, ultrathin sections (80 nm) were cut and contrasted with uranyl acetate and lead citrate. Sections were viewed in the Zeiss EM 10C electron microscope and morphometric analysis was performed as previously described (Gantelet et al., 2007; Panaite et al., 2008). The number of myelinated and unmyelinated axons was counted and the thickness of the myelin sheath calculated (n=7 for each DMSXL and controls).

Analysis of cervical phrenic motor neurons and brainstem respiratory neurons

Serial transverse cryostat sections (20 μm) were prepared from cervical spinal cords (C3-C5) and from brainstems (caudal and rostral to the obex). Sections were either immunolabeled with polyclonal anti-ChAT antibody, which labels motor neurons, or stained with Toluidine Blue. The physical disector method was used to estimate the number of motor neurons in 2-mm segments of either cervical spinal cord or the medullary reticular formation. Identification of respiratory neurons on brainstem sections was achieved according to their localization, as described in several studies (Alheid et al., 2002; Kuwana et al., 2006; Stornetta, 2008). The physical disector method is based on sampling sections, called disector pairs. Four or five disector pairs were used from each animal to estimate the density of neurons, as previously described (Panaite et al., 2011).

Data analysis and statistics

Each respiratory parameter for each mouse (TV, RR, MV, MV/g, heart rate, oxygen saturation) and the data obtained from the diaphragm, phrenic nerves, cervical spinal cord and brainstem examinations were analyzed and compared. ANOVA was used to determine significant difference between the groups, followed by Bonferonni-Holm post-hoc test. Pair-groups were compared by Student's t-test. In all cases, plethysmograph data were normalized to the weight of the animal. Values are reported as mean ± s.d.; P<0.05 was considered a significant difference. All statistical analyses and histograms were performed using GraphPad Prism software (GraphPad Software, La Jolla, CA).

ACKNOWLEDGEMENTS

We wish to thank Dr M. Price for critical reading of the manuscript, and Profs J-P. Hornung and E. Welker for their help in the analysis of the brainstem sections.

COMPETING INTERESTS

The authors declare that they do not have any competing or financial interests.

AUTHOR CONTRIBUTIONS

I.B.-W. conceived and designed the experiments; G.G. generated and provided the DM1 animal model; P.-A.P. and T.K. performed the respiratory tests; P.-A.P. performed animal perfusion, tissue preparation, immunohistochemistry and fluorescence *in situ* hybridization experiments; P.-A.P., J.A.L. and I.B.-W. performed the experiments of histopathological analysis of the diaphragm muscle; P.-A.P., T.K. and I.B.-W. performed the histological analysis of brainstem respiratory neurons, spinal motor neurons, phrenic nerve etc.; P.-A.P. performed statistical analysis. I.B.-W. wrote the paper; P.-A.P., G.G., J.A.L., T.K. and I.B.-W. read the manuscript and approved it.

FUNDING

This work was supported by the Association Française contre les Myopathies [grant number 15644 to I.B.W.].

REFERENCES

Alheid, G. F., Gray, P. A., Jiang, M. C., Feldman, J. L. and McCrimmon, D. R. (2002). Parvalbumin in respiratory neurons of the ventrolateral medulla of the adult rat. *J. Neurocytol.* **31**, 693-717.

Andreose, J. S., Fumagalli, G. and Lømo, T. (1995). Number of junctional acetylcholine receptors: control by neural and muscular influences in the rat. *J. Physiol.* **483**, 397-406.

Ashizawa, T., Dubel, J. R., Dunne, P. W., Dunne, C. J., Fu, Y. H., Pizzuti, A., Caskey, C. T., Boerwinkle, E., Perryman, M. B., Epstein, H. F. et al. (1992). Anticipation in myotonic dystrophy. II. Complex relationships between clinical findings and structure of the GCT repeat. *Neurology* **42**, 1877-1883.

Bégin, R., Bureau, M. A., Lupien, L. and Lemieux, B. (1980). Control and modulation of respiration in Steinert's myotonic dystrophy. *Am. Rev. Respir. Dis.* **121**, 281-289.

Bégin, P., Mathieu, J., Almirall, J. and Grassino, A. (1997). Relationship between chronic hypercapnia and inspiratory-muscle weakness in myotonic dystrophy. *Am. J. Respir. Crit. Care Med.* **156**, 133-139.

Berry, J. K., Vitalo, C. A., Larson, J. L., Patel, M. and Kim, M. J. (1996). Respiratory muscle strength in older adults. *Nurs. Res.* **45**, 154-159.

Bogaard, J. M., van der Meché, F. G., Hendriks, I. and Ververs, C. (1992). Pulmonary function and resting breathing pattern in myotonic dystrophy. *Lung* **170**, 143-153.

Brown, A. G. and Fyffe, R. E. (1978). The morphology of group Ia afferent fibre collaterals in the spinal cord of the cat. *J. Physiol.* **274**, 111-127.

Daubenspeck, J. A., Li, A. and Nattie, E. E. (2008). Acoustic plethysmography measures breathing in unrestrained neonatal mice. *J. Appl. Physiol.* **104**, 262-268.

de Die-Smulders, C. E., Höweler, C. J., Thijs, C., Mirandolle, J. F., Anten, H. B., Smeets, H. J., Chandler, K. E. and Geraedts, J. P. (1998). Age and causes of death in adult-onset myotonic dystrophy. *Brain* **121**, 1557-1563.

Duron, B. and Marlot, D. (1980). The non-myelinated fibers of the phrenic and the intercostal nerves in the cat. *Z. Mikrosk. Anat. Forsch.* **94**, 257-268.

Fodil, R., Lofaso, F., Annane, D., Falaise, L., Lejaille, M., Raphaël, J. C., Isabey, D. and Louis, B. (2004). Upper airway calibre and impedance in patients with Steinert's myotonic dystrophy. *Respir. Physiol. Neurobiol.* **144**, 99-107.

Fu, Y. H., Pizzuti, A., Fenwick, R. G., Jr, King, J., Rajnarayan, S., Dunne, P. W., Dubel, J., Nasser, G. A., Ashizawa, T., de Jong, P. et al. (1992). An unstable triplet repeat in a gene related to myotonic muscular dystrophy. *Science* **255**, 1256-1258.

Gantelet, E., Kraftsik, R., Delaloye, S., Gourdon, G., Kuntzer, T. and Barakat-Walter, I. (2007). The expansion of 300 CTG repeats in myotonic dystrophy transgenic mice does not induce sensory or motor neuropathy. *Acta Neuropathol.* **114**, 175-185.

Gennarelli, M., Novelli, G., Andreasi Bassi, F., Martorell, L., Cornet, M., Menegazzo, E., Mostacciuolo, M. L., Martinez, J. M., Angelini, C., Pizzuti, A. et al. (1996). Prediction of myotonic dystrophy clinical severity based on the number of intragenic [CTG]n trinucleotide repeats. *Am. J. Med. Genet.* **65**, 342-347.

Gomes-Pereira, M., Foiry, L., Nicole, A., Huguet, A., Junien, C., Munnich, A. and Gourdon, G. (2007). CTG trinucleotide repeat "big jumps": large expansions, small mice. *PLoS Genet.* **3**, e52.

Gomes-Pereira, M., Cooper, T. A. and Gourdon, G. (2011). Myotonic dystrophy mouse models: towards rational therapy development. *Trends Mol. Med.* **17**, 506-517.

Goshgarian, H. G. and Roubal, P. J. (1986). Origin and distribution of phrenic primary afferent nerve fibers in the spinal cord of the adult rat. *Exp. Neurol.* **92**, 624-638.

Groh, W. J., Groh, M. R., Saha, C., Kincaid, J. C., Simmons, Z., Ciafaloni, E., Pourmand, R., Otten, R. F., Bhakta, D., Nair, G. V. et al. (2008). Electrocardiographic abnormalities and sudden death in myotonic dystrophy type 1. *N. Engl. J. Med.* **358**, 2688-2697.

Guido, A. N., Campos, G. E., Neto, H. S., Marques, M. J. and Minatel, E. (2010). Fiber type composition of the sternomastoid and diaphragm muscles of dystrophin-deficient mdx mice. *Anat. Rec. (Hoboken)* **293**, 1722-1728.

Guiraud-Dogan, C., Huguet, A., Gomes-Pereira, M., Brisson, E., Bassez, G., Junien, C. and Gourdon, G. (2007). DM1 CTG expansions affect insulin receptor isoforms expression in various tissues of transgenic mice. *Biochim. Biophys. Acta* **1772**, 1183-1191.

Hamelmann, E., Schwarze, J., Takeda, K., Oshiba, A., Larsen, G. L., Irvin, C. G. and Gelfand, E. W. (1997). Noninvasive measurement of airway responsiveness in allergic mice using barometric plethysmography. *Am. J. Respir. Crit. Care Med.* **156**, 766-775.

Harper, P. S. (1989). Gene mapping and the muscular dystrophies. *Prog. Clin. Biol. Res.* **306**, 29-49.
Harper, P. S. (2001). *Myotonic Dystrophy*, 3rd edn. London, UK: Saunders WB.
Hoymann, H. G. (2007). Invasive and noninvasive lung function measurements in rodents. *J. Pharmacol. Toxicol. Methods* **55**, 16-26.
Huang, P., Cheng, G., Lu, H., Aronica, M., Ransohoff, R. M. and Zhou, L. (2011). Impaired respiratory function in mdx and mdx/utrn(+/-) mice. *Muscle Nerve* **43**, 263-267.
Huguet, A., Medja, F., Nicole, A., Vignaud, A., Guiraud-Dogan, C., Ferry, A., Decostre, V., Hogrel, J. Y., Metzger, F., Hoeflich, A. et al. (2012). Molecular, physiological, and motor performance defects in DMSXL mice carrying >1,000 CTG repeats from the human DM1 locus. *PLoS Genet.* **8**, e1003043.
Hunter, A., Tsilfidis, C., Mettler, G., Jacob, P., Mahadevan, M., Surh, L. and Korneluk, R. (1992). The correlation of age of onset with CTG trinucleotide repeat amplification in myotonic dystrophy. *J. Med. Genet.* **29**, 774-779.
Jammes, Y., Pouget, J., Grimaud, C. and Serratrice, G. (1985). Pulmonary function and electromyographic study of respiratory muscles in myotonic dystrophy. *Muscle Nerve* **8**, 586-594.
Jammes, Y., Buchler, B., Delpierre, S., Rasidakis, A., Grimaud, C. and Roussos, C. (1986). Phrenic afferents and their role in inspiratory control. *J. Appl. Physiol.* **60**, 854-860.
Jaspert, A., Fahsold, R., Grehl, H. and Claus, D. (1995). Myotonic dystrophy: correlation of clinical symptoms with the size of the CTG trinucleotide repeat. *J. Neurol.* **242**, 99-104.
Kilburn, K. H., Eagan, J. T., Sieker, H. O. and Heyman, A. (1959). Cardiopulmonary insufficiency i myotonic and progressive muscular dystrophy. *N. Engl. J. Med.* **261**, 1089-1096.
Kumai, Y., Ito, T., Matsukawa, A. and Yumoto, E. (2005). Effects of denervation on neuromuscular junctions in the thyroarytenoid muscle. *Laryngoscope* **115**, 1869-1872.
Kumazawa, T. and Mizumura, K. (1977). Thin-fibre receptors responding to mechanical, chemical, and thermal stimulation in the skeletal muscle of the dog. *J. Physiol.* **273**, 179-194.
Kuwana, S., Tsunekawa, N., Yanagawa, Y., Okada, Y., Kuribayashi, J. and Obata, K. (2006). Electrophysiological and morphological characteristics of GABAergic respiratory neurons in the mouse pre-Bötzinger complex. *Eur. J. Neurosci.* **23**, 667-674.
Kuyumcu-Martinez, N. M. and Cooper, T. A. (2006). Misregulation of alternative splicing causes pathogenesis in myotonic dystrophy. *Prog. Mol. Subcell. Biol.* **44**, 133-159.
Langford, L. A. and Schmidt, R. F. (1983). An electron microscopic analysis of the left phrenic nerve in the rat. *Anat. Rec.* **205**, 207-213.
Larnicol, N., Rose, D. and Duron, B. (1985). Identification of phrenic afferents to the external cuneate nucleus: a fluorescent double-labeling study in the cat. *Neurosci. Lett.* **62**, 163-167.
Macron, J. M., Marlot, D. and Duron, B. (1985). Phrenic afferent input to the lateral medullary reticular formation of the cat. *Respir. Physiol.* **59**, 155-167.
Mahadevan, M., Tsilfidis, C., Sabourin, L., Shutler, G., Amemiya, C., Jansen, G., Neville, C., Narang, M., Barceló, J., O'Hoy, K. et al. (1992). Myotonic dystrophy mutation: an unstable CTG repeat in the 3 untranslated region of the gene. *Science* **255**, 1253-1255.
Marchini, C., Lonigro, R., Verriello, L., Pellizzari, L., Bergonzi, P. and Damante, G. (2000). Correlations between individual clinical manifestations and CTG repeat amplification in myotonic dystrophy. *Clin. Genet.* **57**, 74-82.
Marlon, D. and Duron, B. (1981). Postnatal development of the discharge pattern of phrenic motor units in the kitten. *Respir. Physiol.* **46**, 125-136.
Marlot, D., Macron, J. M. and Duron, B. (1988). Effects of ipsilateral and contralateral cervical phrenic afferents stimulation on phrenic motor unit activity in the cat. *Brain Res.* **450**, 373-377.
Marteyn, A., Maury, Y., Gauthier, M. M., Lecuyer, C., Vernet, R., Denis, J. A., Pietu, G., Peschanski, M. and Martinat, C. (2011). Mutant human embryonic stem cells reveal neurite and synapse formation defects in type 1 myotonic dystrophy. *Cell Stem Cell* **8**, 434-444.
Mathieu, J., Allard, P., Potvin, L., Prévost, C. and Bégin, P. (1999). A 10-year study of mortality in a cohort of patients with myotonic dystrophy. *Neurology* **52**, 1658-1662.
Mead, J., Jeffrey, C. S. and Loring, S. H. (1995). Volume displacements of the chest wall and their mechanical significanc. In *The Thorax: Physiology* (ed. C. Roussos), pp. 565-586. New York, NY: Marcel Dekker.
Nykamp, K. R. and Swanson, M. S. (2008). Toxic RNA in the nucleus: unstable microsatellite expression in neuromuscular disease. *Prog. Mol. Subcell. Biol.* **35**, 57-77.
Ogawa, K., Iranami, H., Yoshiyama, T., Maeda, H. and Hatano, Y. (1993). Severe respiratory depression after epidural morphine in a patient with myotonic dystrophy. *Can. J. Anaesth.* **40**, 968-970.
Ono, S., Kanda, F., Takahashi, K., Fukuoka, Y., Jinnai, K., Kurisaki, H., Mitake, S., Inagaki, T. and Nagao, K. (1996). Neuronal loss in the medullary reticular formation in myotonic dystrophy: a clinicopathological study. *Neurology* **46**, 228-231.
Panaite, P. A., Gantelet, E., Kraftsik, R., Gourdon, G., Kuntzer, T. and Barakat-Walter, I. (2008). Myotonic dystrophy transgenic mice exhibit pathologic abnormalities in diaphragm neuromuscular junctions and phrenic nerves. *J. Neuropathol. Exp. Neurol.* **67**, 763-772.
Panaite, P. A., Kielar, M., Kraftsik, R., Gourdon, G., Kuntzer, T. and Barakat-Walter, I. (2011). Peripheral neuropathy is linked to a severe form of myotonic dystrophy in transgenic mice. *J. Neuropathol. Exp. Neurol.* **70**, 678-685.
Petrof, B. J., Stedman, H. H., Shrager, J. B., Eby, J., Sweeney, H. L. and Kelly, A. M. (1993). Adaptations in myosin heavy chain expression and contractile function in dystrophic mouse diaphragm. *Am. J. Physiol.* **265**, C834-C841.
Querido, E., Gallardo, F., Beaudoin, M., Ménard, C. and Chartrand, P. (2011). Stochastic and reversible aggregation of mRNA with expanded CUG-triplet repeats. *J. Cell Sci.* **124**, 1703-1714.
Ramirez, J. M., Zuperku, E. J., Alheid, G. F., Lieske, S. P., Ptak, K. and McCrimmon, D. R. (2002). Respiratory rhythm generation: converging concepts from in vitro and in vivo approaches? *Respir. Physiol. Neurobiol.* **131**, 43-56.
Reardon, W., Newcombe, R., Fenton, I., Sibert, J. and Harper, P. S. (1993). The natural history of congenital myotonic dystrophy: mortality and long term clinical aspects. *Arch. Dis. Child.* **68**, 177-181.
Revelette, W. R., Jewell, L. A. and Frazier, D. T. (1988). Effect of diaphragm small-fiber afferent stimulation on ventilation in dogs. *J. Appl. Physiol.* **65**, 2097-2106.
Romeo, V. (2012). Myotonic Dystrophy Type 1 or Steinert's disease. *Adv. Exp. Med. Biol.* **724**, 239-257.
Salehi, L. B., Bonifazi, E., Stasio, E. D., Gennarelli, M., Botta, A., Vallo, L., Iraci, R., Massa, R., Antonini, G., Angelini, C. et al. (2007). Risk prediction for clinical phenotype in myotonic dystrophy type 1: data from 2,650 patients. *Genet. Test.* **11**, 84-90.
Serisier, D. E., Mastaglia, F. L. and Gibson, G. J. (1982). Respiratory muscle function and ventilatory control. I in patients with motor neurone disease. II in patients with myotonic dystrophy. *Q. J. Med.* **51**, 205-226.
Seznec, H., Agbulut, O., Sergeant, N., Savouret, C., Ghestem, A., Tabti, N., Willer, J. C., Ourth, L., Duros, C., Brisson, E. et al. (2001). Mice transgenic for the human myotonic dystrophy region with expanded CTG repeats display muscular and brain abnormalities. *Hum. Mol. Genet.* **10**, 2717-2726.
Sheehan, D. C. and Hrapchak, B. B. (1980). *Theory and Practice of Histotechnology*, 2nd edn. St Louis, MO: Mosby.
Singh, B., Panizza, J. A. and Finucane, K. E. (2003). Breath-by-breath measurement of the volume displaced by diaphragm motion. *J. Appl. Physiol.* **94**, 1084-1091.
Speck, D. F. and Revelette, W. R. (1987). Excitation of dorsal and ventral respiratory group neurons by phrenic nerve afferents. *J. Appl. Physiol.* **62**, 946-951.
Stornetta, R. L. (2008). Identification of neurotransmitters and co-localization of transmitters in brainstem respiratory neurons. *Respir. Physiol. Neurobiol.* **164**, 18-27.
Stunden, C. E., Filosa, J. A., Garcia, A. J., Dean, J. B. and Putnam, R. W. (2001). Development of in vivo ventilatory and single chemosensitive neuron responses to hypercapnia in rats. *Respir. Physiol.* **127**, 135-155.
Takasugi, T., Ishihara, T., Kawamura, J. and Kawashiro, T. (1995). [Respiratory failure: respiratory disorder during sleep in patients with myotonic dystrophy]. *Rinsho Shinkeigaku* **35**, 1486-1488.
Takezawa, J., Miller, F. J. and O'Neil, J. J. (1980). Single-breath diffusing capacity and lung volumes in small laboratory mammals. *J. Appl. Physiol.* **48**, 1052-1059.
Wansink, D. G. and Wieringa, B. (2003). Transgenic mouse models for myotonic dystrophy type 1 (DM1). *Cytogenet. Genome Res.* **100**, 230-242.
Wheeler, T. M., Krym, M. C. and Thornton, C. A. (2007). Ribonuclear foci at the neuromuscular junction in myotonic dystrophy type 1. *Neuromuscul. Disord.* **17**, 242-247.
Yilmaz, C., Johnson, R. L., Jr and Hsia, C. C. (2005). A rebreathing method for measuring lung volume, diffusing capacity and cardiac output in conscious small animals. *Respir. Physiol. Neurobiol.* **146**, 215-223.
Yomosa, H., Nakahashi, K., Hayashi, M., Marunaka, S., Yan, S. and Hiraki, N. (1991). [General anesthesia with sevoflurane and vecuronium for patients with dystrophia myotonica and progressive muscular dystrophy]. *Masui* **40**, 1730-1735.
Zifko, U. A., Hahn, A. F., Remtulla, H., George, C. F., Wihlidal, W. and Bolton, C. F. (1996). Central and peripheral respiratory electrophysiological studies in myotonic dystrophy. *Brain* **119**, 1911-1922.